SUPPORTING INFORMATION

Unprecedented *pseudo* zeroth order kinetics of catecholase-like activity of mixed valence $Mn^{II}Mn_2^{III}$ complexes

Sanchari Dasgupta,*[,a,b] Suhana Karim,[a] Somanjana Khatua,[c] Amit Adhikary,[a] Krishnendu Acharya,[c] Ennio Zangrando,[d] Suvendu Maity,[e] Debasis Das *[,a]

[a] Department of Chemistry, University of Calcutta, 92, A. P. C. Road, Kolkata 700009, India

[b] Institut Lavoisier de Versailles, UMR CNRS 8180, Université de Versailles St-Quentin-en-Yvelines, Université Paris-Saclay, 78035 Versailles Cedex, France

[c] Molecular and Applied Mycology and Plant Pathology Laboratory, Centre of Advanced Study, Department of Botany, University of Calcutta, 35, Ballygunge Circular Road, Kolkata 700019, India

[d] Department of Chemical and Pharmaceutical Sciences, University of Trieste, Via L. Giorgieri 1, 34127 Trieste, Italy

[e] Department of Chemistry, R. K. Mission Residential College, Narendrapur, Kolkata 700103, India

Table S1. Selected bond distances (Å) and angles (°) for complex **1.**

Mn(1)-O(1)	1.884(3)	Mn(3)-O(2)	1.881(3)
Mn(1)-N(1)	2.005(4)	Mn(3)-N(2)	1.992(4)
Mn(1)-O(3)	1.865(3)	Mn(3)-O(4)	1.881(3)
Mn(1)-O(11)	1.956(4)	Mn(3)-O(7)	1.936(4)
Mn(1)-O(9)	2.183(3)	Mn(3)-O(5)	2.217(3)
Mn(1)-O(1w)	2.317(4)	Mn(3)-O(2w)	2.329(4)
Mn(2)-O(3)	2.157(3)	Mn(2)-O(8)	2.139(4)
Mn(2)-O(4)	2.143(3)	Mn(2)-O(10)	2.197(4)
Mn(2)-O(6)	2.186(4)	Mn(2)-O(12)	2.132(4)

Table S2. Selected bond distances (Å) and angles (°) for complex **2.**

Mn(1)-O(1)	1.8960(14)	Mn(1)-O(3)	2.3216(11)
Mn(1)-N(1)	2.0060(13)	Mn(2)-O(2)	2.1177(10)
Mn(1)-O(2)	1.8714(13)	Mn(2)-O(5)	2.2102(11)
Mn(1)-O(6)	1.9471(12)	Mn(2)-O(7)	2.1476(12)
Mn(1)-O(4)	2.1775(10)		

Table S3. Coordination bond angles (°) for compounds **1-2.**

Complex 1			
O(3)-Mn(1)-O(1)	174.11(15)	O(4)-Mn(2)-O(6)	90.08(13)
O(3)-Mn(1)-O(11)	96.69(14)	O(3)-Mn(2)-O(6)	87.18(13)
O(1)-Mn(1)-O(11)	89.00(15)	O(12)-Mn(2)-O(10)	91.68(15)
O(3)-Mn(1)-N(1)	82.91(15)	O(8)-Mn(2)-O(10)	88.86(16)
O(1)-Mn(1)-N(1)	91.21(16)	O(4)-Mn(2)-O(10)	91.19(13)
O(11)-Mn(1)-N(1)	167.36(15)	O(3)-Mn(2)-O(10)	91.56(13)
O(3)-Mn(1)-O(9)	93.16(13)	O(6)-Mn(2)-O(10)	178.48(15)
O(1)-Mn(1)-O(9)	87.76(14)	O(2)-Mn(3)-O(4)	174.04(14)
O(11)-Mn(1)-O(9)	95.70(14)	O(2)-Mn(3)-O(7)	86.25(15)
N(1)-Mn(1)-O(9)	96.94(15)	O(4)-Mn(3)-O(7)	98.82(14)
O(3)-Mn(1)-O(1w)	90.37(15)	O(2)-Mn(3)-N(2)	91.36(16)
O(1)-Mn(1)-O(1w)	89.02(15)	O(4)-Mn(3)-N(2)	83.24(15)
O(11)-Mn(1)-O(1w)	81.06(15)	O(7)-Mn(3)-N(2)	173.13(15)
N(1)-Mn(1)-O(1w)	86.31(16)	O(2)-Mn(3)-O(5)	89.82(13)
O(9)-Mn(1)-O(1w)	175.47(14)	O(4)-Mn(3)-O(5)	93.13(13)
O(12)-Mn(2)-O(8)	176.99(13)	O(7)-Mn(3)-O(5)	91.68(14)
O(12)-Mn(2)-O(4)	91.80(13)	N(2)-Mn(3)-O(5)	94.76(15)
O(8)-Mn(2)-O(4)	91.15(13)	O(2)-Mn(3)-O(2w)	90.01(14)
O(12)-Mn(2)-O(3)	87.72(13)	O(4)-Mn(3)-O(2w)	87.38(14)
O(8)-Mn(2)-O(3)	89.30(13)	O(7)-Mn(3)-O(2w)	84.51(15)
O(4)-Mn(2)-O(3)	177.22(13)	N(2)-Mn(3)-O(2w)	89.05(15)
O(12)-Mn(2)-O(6)	89.10(15)	O(5)-Mn(3)-O(2w)	176.19(14)
O(8)-Mn(2)-O(6)	90.29(16)		

Complex 2			
O(2)-Mn(1)-O(1)	173.18(4)	O(6)-Mn(1)-O(3)	81.76(4)
O(2)-Mn(1)-O(6)	95.62(5)	N(1)-Mn(1)-O(3)	86.22(5)
O(1)-Mn(1)-O(6)	90.09(5)	O(4)-Mn(1)-O(3)	176.83(4)
O(2)-Mn(1)-N(1)	82.97(5)	O(2)-Mn(2)-O(2’)	180.0
O(1)-Mn(1)-N(1)	90.68(5)	O(5)-Mn(2)-O(5’)	180.0
O(6)-Mn(1)-N(1)	167.97(4)	O(7’)-Mn(2)-O(7’)	180.0
O(2)-Mn(1)-O(4)	94.40(4)	O(2)-Mn(2)-O(7)	88.19(5)
O(1)-Mn(1)-O(4)	88.80(5)	O(2)-Mn(2)-O(7’)	91.81(5)
O(6)-Mn(1)-O(4)	95.12(4)	O(2)-Mn(2)-O(5)	93.53(5)
N(1)-Mn(1)-O(4)	96.90(4)	O(2)-Mn(2)-O(5’)	86.47(5)
O(2)-Mn(1)-O(3)	86.49(5)	O(7)-Mn(2)-O(5)	90.70(5)
O(1)-Mn(1)-O(3)	90.64(5)	O(7)-Mn(2)-O(5’)	89.30(5)

Primed atoms. at 1-x, -y, 1-z.

Table S4. H-bonding parameters for complexes **1** and **2**

Complex 1						
D-H	d(D-H)	d(H..A)	d(D..A)	d(D..A)	A	Symmetry
O(1w)-H(21)	0.75(8)	2.01(8)	2.750(12)	171(8)	O(7w)	1-x, 1-y, 1-z
O(1w)-H(22)	0.77(7)	1.95(7)	2.713(7)	174(7)	O(6w)	1+x, y, z
O(2w)-H(11)	0.86(5)	2.00(5)	2.852(7)	172(3)	O(3w)	2-x, -y, -z
O(2w)-H(12)	0.83(4)	1.99(4)	2.816(6)	178(8)	O(3w)	
O(3w)-H(31)	0.85(4)	1.99(4)	2.838(5)	175(7)	O(10)	
O(3w)-H(32)	0.85(5)	2.07(4)	2.869(6)	155(6)	O(4w)	1-x, 1-y, -z
O(4w)-H(41)	0.84(6)	2.23(5)	3.056(6)	168(7)	O(9)	-1+x, y, z
O(4w)-H(42)	0.83(7)	2.42(7)	3.127(6)	144(7)	O(2)	-1+x, 1+y, z
O(5w)-H(51)	0.84(7)	2.33(6)	3.026(7)	141(6)	O(11)	
O(5w)-H(52)	0.83(4)	2.02(4)	2.854(67)	180(11)	O(5)	x, 1+y, z
O(6w)-H(61)	0.81(7)	2.04(7)	2.843(6)	177(10)	O(6)	1-x, 1-y, 1-z
O(6w)-H(62)	0.75(6)	2.21(6)	2.948(7)	170(9)	O(1w)	1-x, 1-y,1-z
O(7w)-H(71)	0.92(12)	1.89(14)	2.673(9)	142(13)	O(5w)	1-x, 1-y, 1-z
O(7w)-H(72)	0.72(11)				-	
Complex 2						
O(1s)-H(1s)	0.82	2.01	2.806(2)	162	O(5)	1-x,-y,1-z
O(2s)-H(2s)	0.82	2.09	2.890(3)	166	O(4)	
O(3)-H(3a)	0.82(2)	1.89(2)	2.707(2)	176.3(17)	O(1s)	

Table S5. Details of X-band EPR experiments for complexes **1** and **2**

Complex	**conditions**	**microwave frequency**	**modulation amplitude (mT)**	**BO-Sweep (mT)**	**sweep rate (S)**
1	77 K, acetonitrile solution	9.4429	200	599.6	60
1	solid state	9.4347	200	599.6	60
1	77 K, methanol medium	9.4431	200	399.46	120
1	1:1(v/v) methanol-water	9.4434	200	399.46	120
2	77 K, acetonitrile solution	9.4437	200	499.4	60
2	solid state	9.4447	200	499.4	60
2	77 K, methanol medium	9.4413	200	399.46	120
2	1:1 (v/v) methanol-water	9.4486	200	399.46	120

Table S6. The rate (M min^{-1}) of the complexes for catecholase-like activity at a concentration higher than 600 equivalents.

Catalyst : Substrate Molar ratio	Complex **1**	Complex **2**
1 : 700	1.56×10^{-7}	1.62×10^{-7}
1 : 800	1.13×10^{-7}	1.39×10^{-7}
1 : 900	1.01×10^{-7}	7.56×10^{-8}

Table S7. Initial rate (M min^{-1}) and the overall rate (M min^{-1}) of complexes **1** and **2** for pseudo zero order kinetics of catecholase-like activity in acetonitrile medium. The rates were obtained by dividing individual slopes and molar extinction coefficient (ϵ) of 3,5-DTBQ.

Catalyst: Substrate Molar ratio	Complex **1**		Complex **2**	
	Initial Rate	Overall Rate	Initial Rate	Overall Rate
1:100	4.21×10^{-6}	3.16×10^{-6}	4.22×10^{-6}	3.17×10^{-6}
1:200	5.37×10^{-6}	3.28×10^{-6}	5.36×10^{-6}	3.29×10^{-6}
1:300	5.74×10^{-6}	3.49×10^{-6}	5.95×10^{-6}	3.24×10^{-6}
1:400	6.21×10^{-6}	3.59×10^{-6}	6.37×10^{-6}	3.31×10^{-6}
1:500	6.42×10^{-6}	3.72×10^{-6}	6.84×10^{-6}	3.30×10^{-6}
1:600	6.89×10^{-6}	3.67×10^{-6}	6.90×10^{-6}	3.46×10^{-6}

Table S8. Crystal data and details of structure refinements for compounds **1-2**.

	1	**2**
CCDC Number	1916631	1916632
Empirical formula	$C_{30}H_{50}Br_2Mn_3N_2O_{19}$	$C_{35}H_{54}Br_4Mn_3N_2O_{17}$
Formula weight	1067.36	1259.26
Crystal system	Triclinic	Triclinic
Space group	$P\bar{1}$	$P\bar{1}$
a (Å)	10.981(5)	8.2310(16)
b (Å)	11.954(5)	12.816(3)
c (Å)	17.826(5)	13.335(3)
α (deg)	100.945(5)	61.78(3)
β (deg)	90.352(5)	85.43(3)
γ (deg)	108.241(5)	73.33(3)
Volume ($Å^3$)	2176.5(15)	1184.9(5)
Z	2	1
D_{calcd} (g cm^{-3})	1.629	1.765
μ Mo-Kα, (mm^{-1})	2.765	3.972
F(000)	1082	627
θ_{max} (°)	25.15	29.71
Reflns collected	31467	24638
Unique reflections	7641	7015
R_{int}	0.0738	0.0521
Observed $I > 2\sigma(I)$	4840	6833
Parameters	555	296
Goodness of fit (F^2)	1.035	1.159
$R1$/ $wR2$ ($I > 2\sigma(I)$) [a]	0.0484/ 0.1046	0.0271/ 0.0657
Δρ (e/$Å^3$)	0.733, –0.577	0.538, –1.089

[a] $R1 = \Sigma \big| |Fo| - |Fc| \big| / \Sigma |Fo|$, $wR2 = [\Sigma w (Fo^2 - Fc^2)^2 / \Sigma w (Fo^2)^2]^{½}$

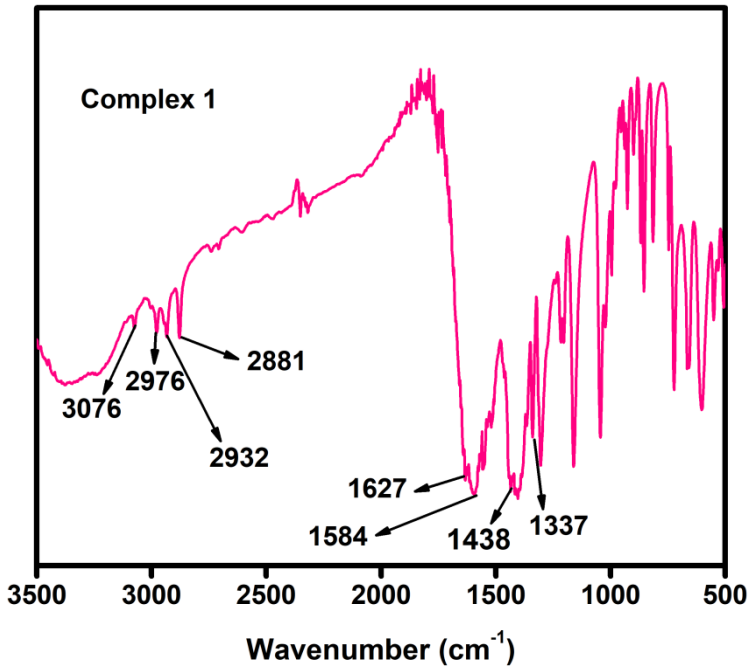

Fig. S1. FT-IR spectrum of complex **1**.

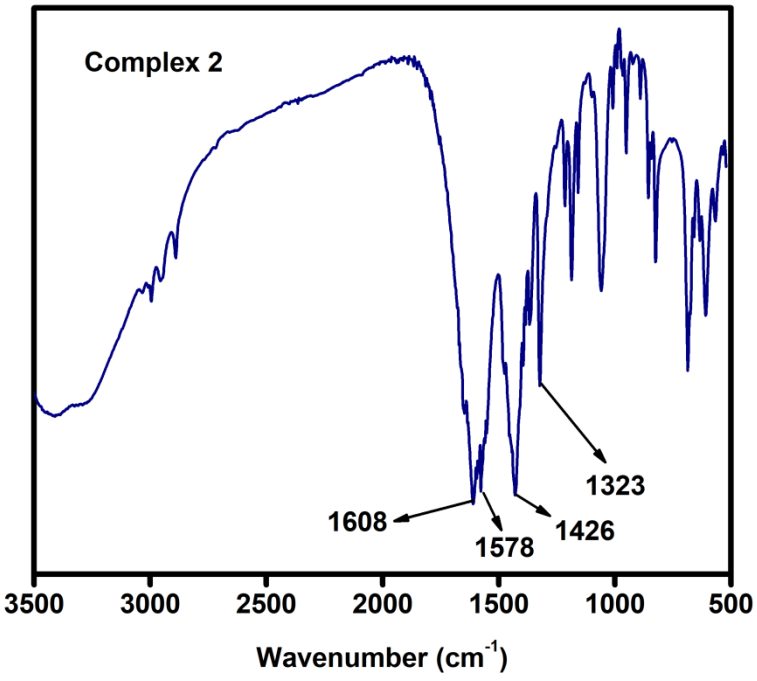

Fig. S2. FT-IR spectrum of complex **2**.

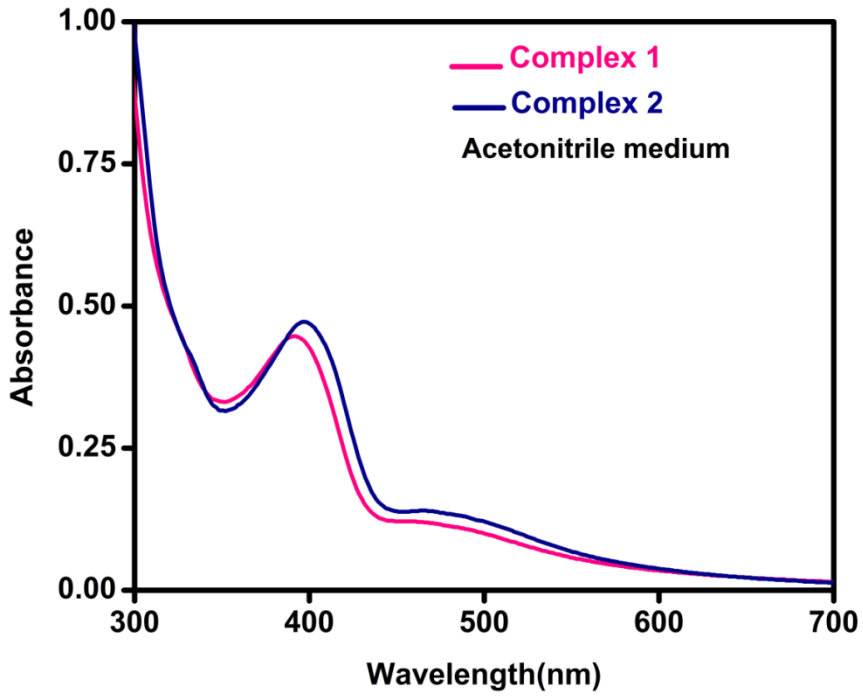

Fig. S3. UV-Vis spectra of complexes **1** and **2** in acetonitrile medium.

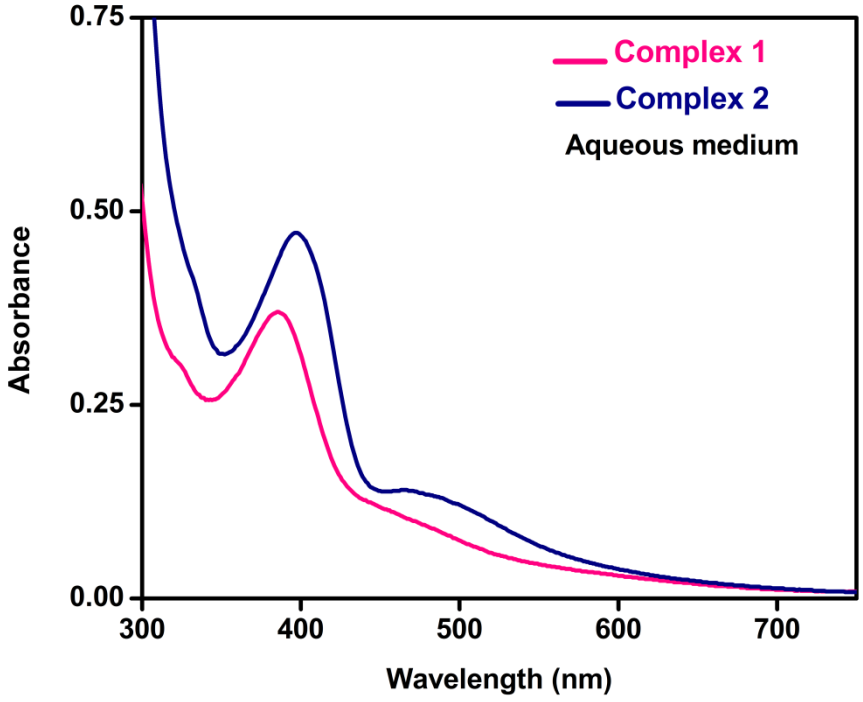

Fig. S4. UV-Vis spectra of complexes **1** and **2** in aqueous medium.

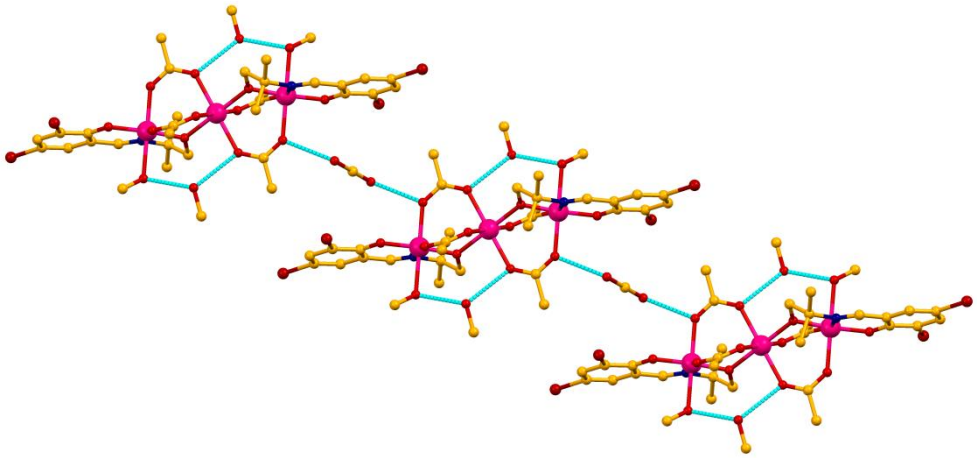

Fig. S5. Hydrogen bonding interactions in complex **2** viewed along b axis.

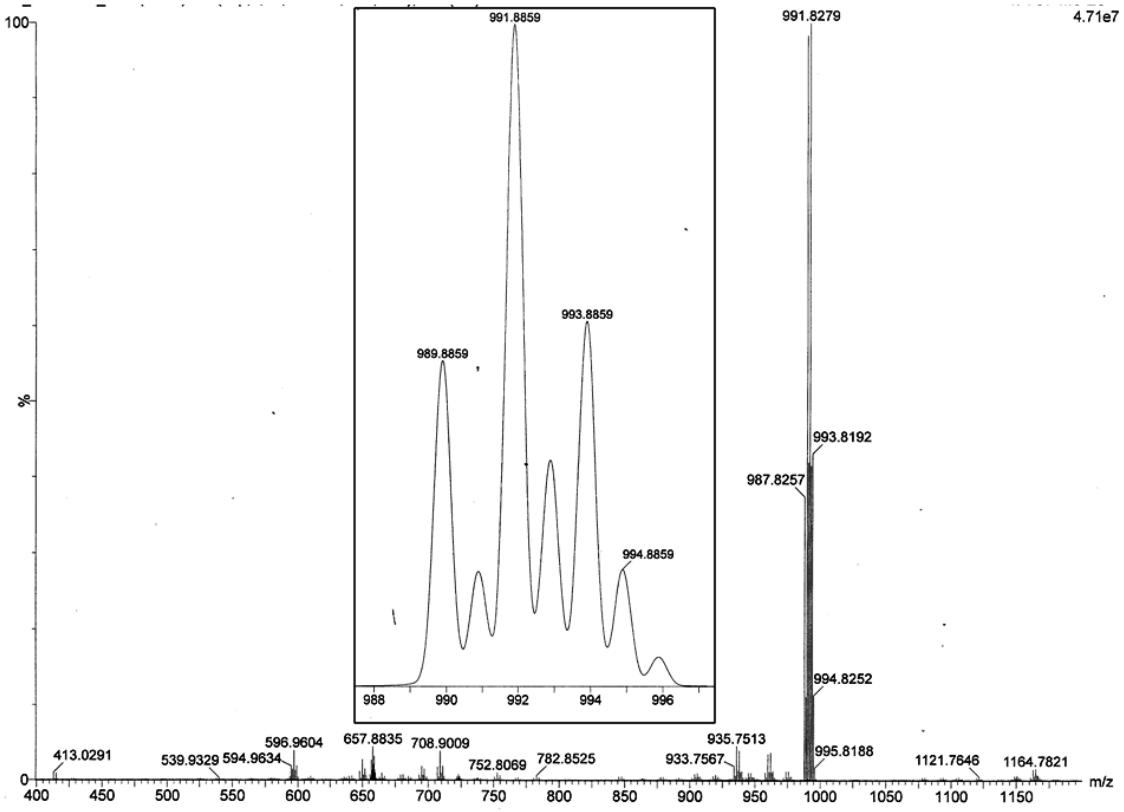

Fig. S6. ESI-MS spectrum of complex **1** in acetonitrile medium.

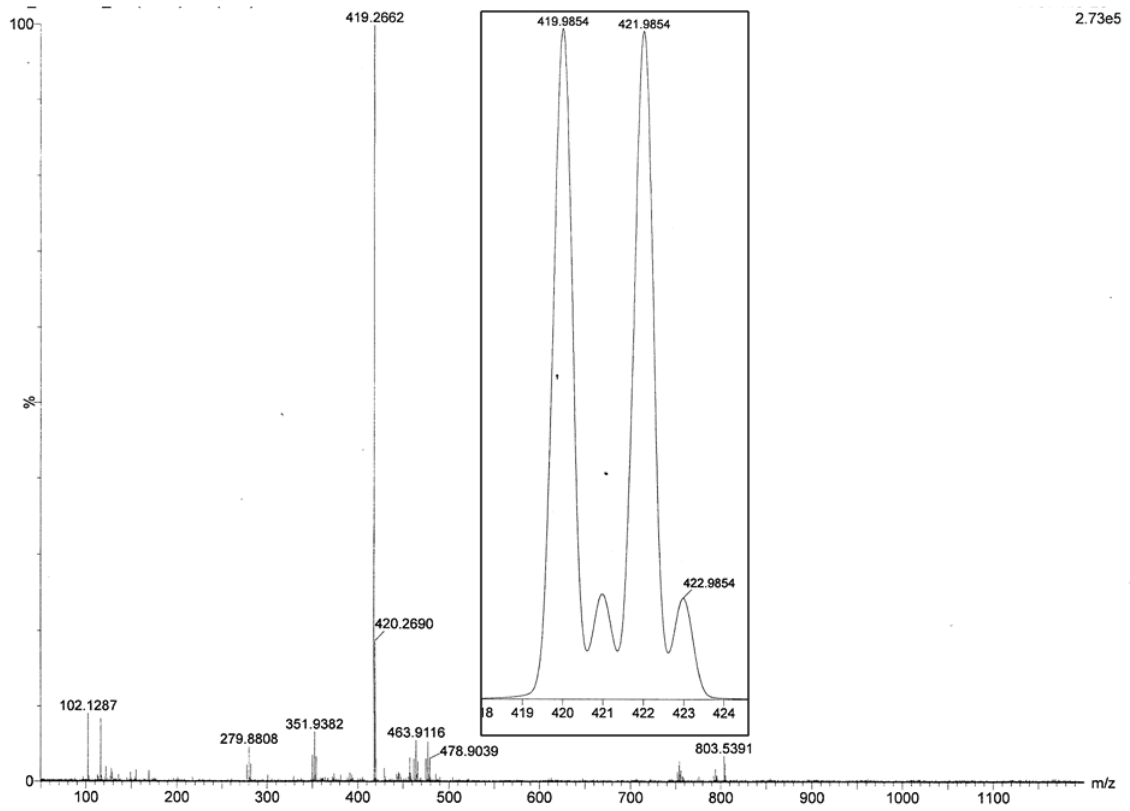

Fig. S7. ESI-MS spectrum of complex **1** in an aqueous medium.

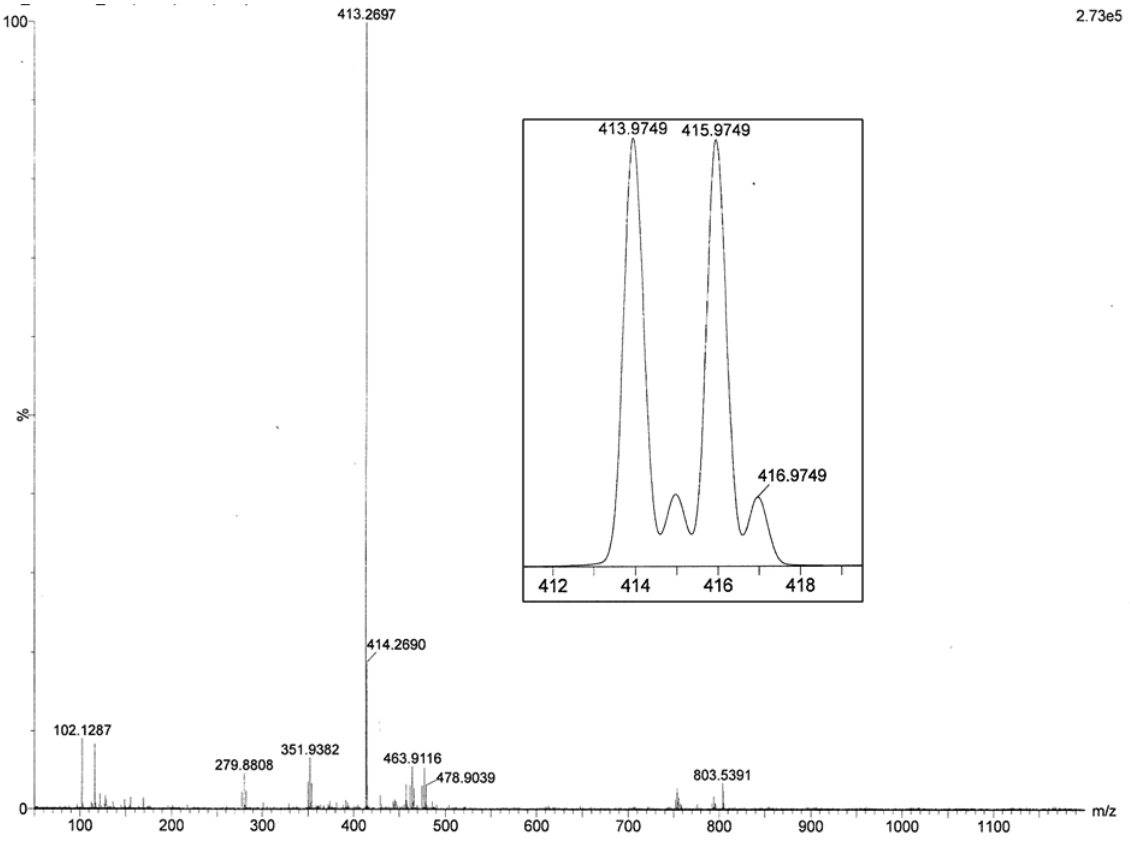

Fig. S8. ESI-MS spectrum of complex **1** in methanol medium.

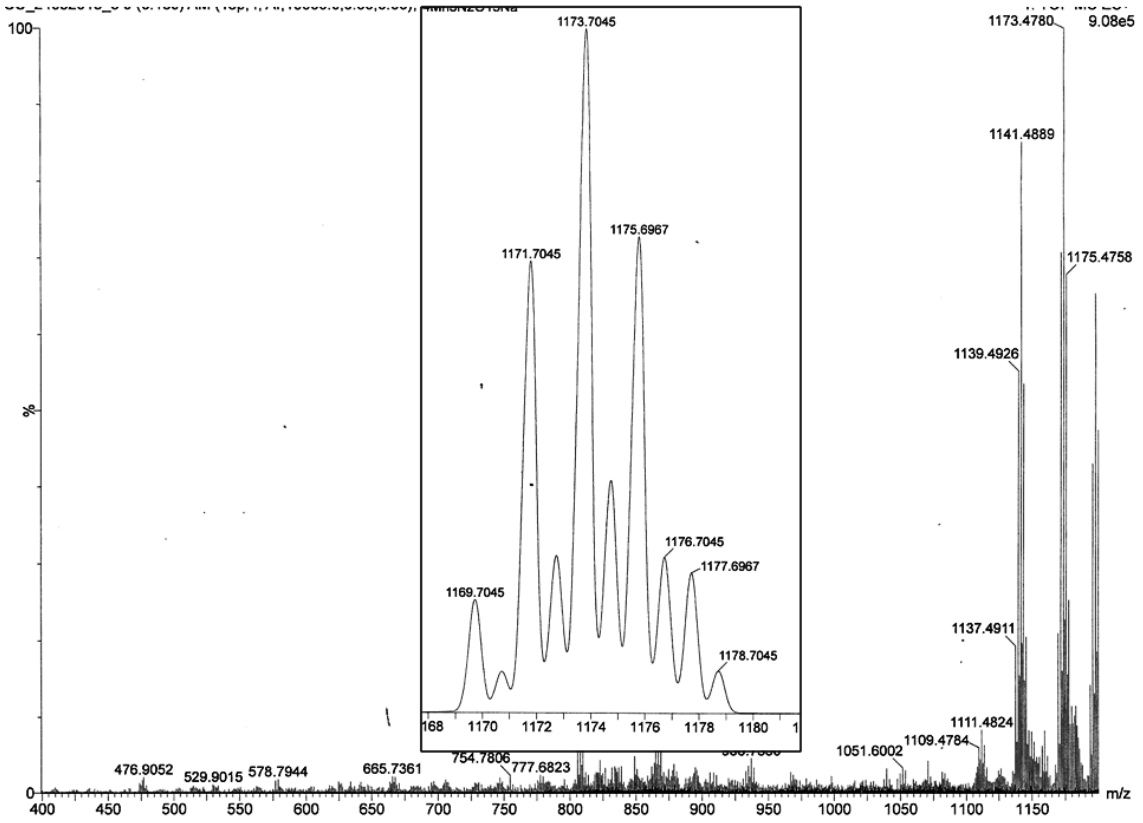

Fig. S9. ESI-MS spectrum of complex **2** in acetonitrile medium.

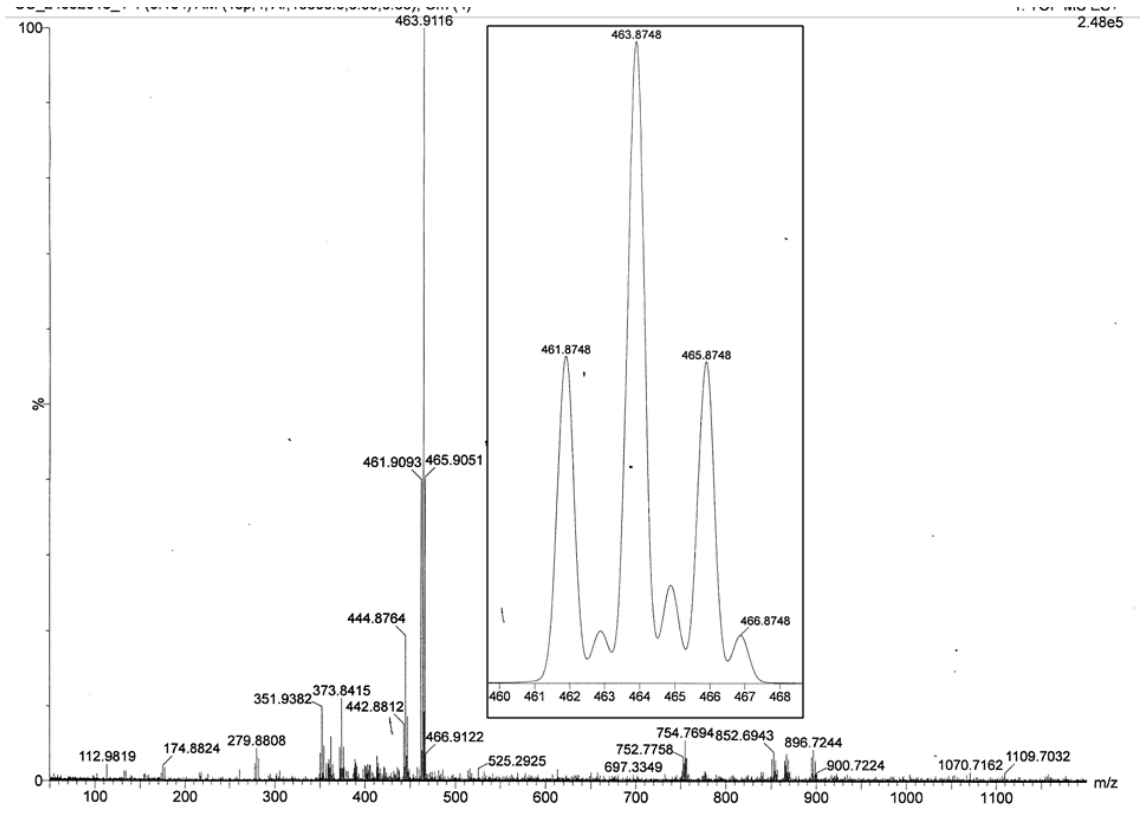

Fig. S10 ESI-MS spectrum of complex **2** in an aqueous medium.

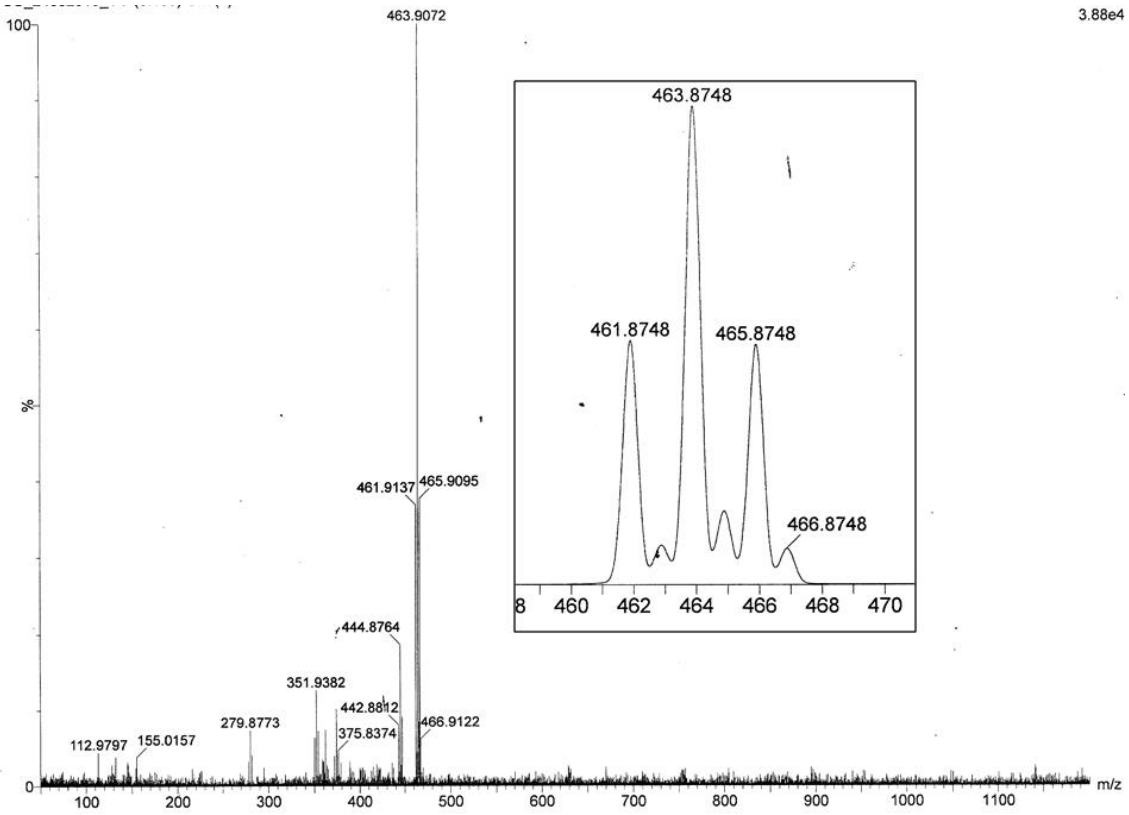

Fig. S11 ESI-MS spectrum of complex **2** in methanol medium.

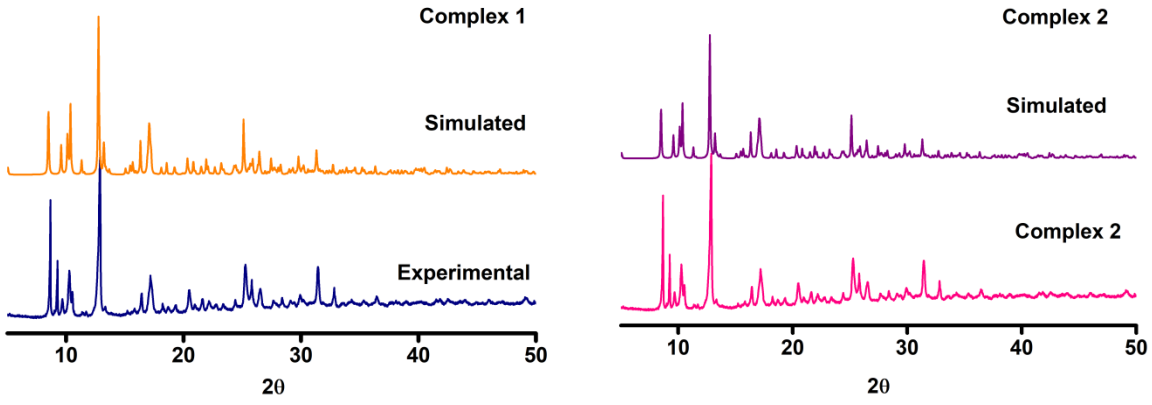

(a) (b)

Fig. S12. Powder X-ray diffraction pattern of (a) complex **1** and (b) complex **2.**

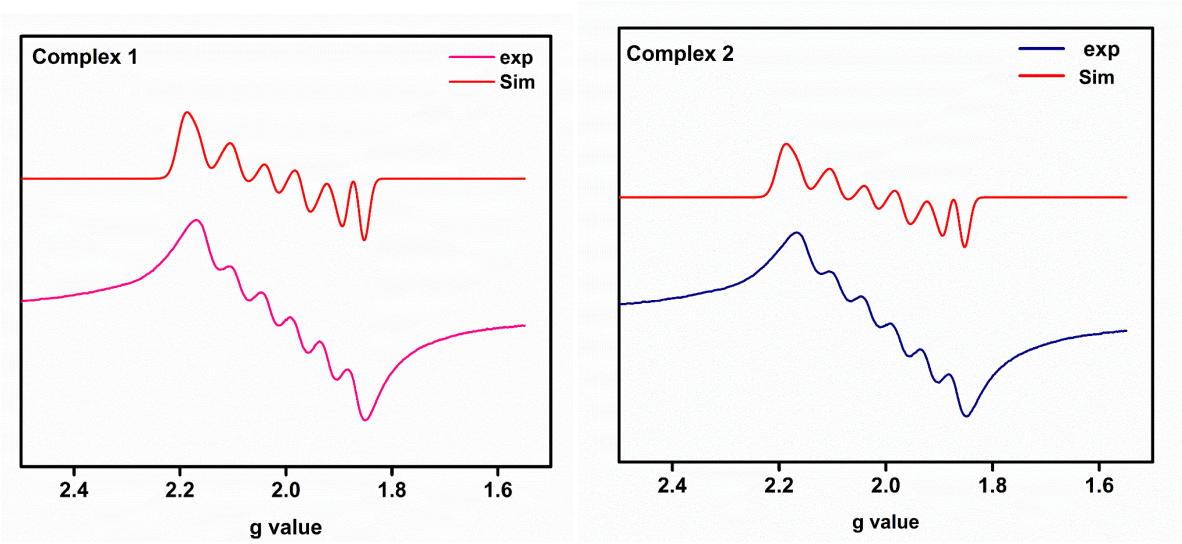

Fig. S13. X-Band EPR spectra of complexes **1** and **2** in methanol medium at 77 K.

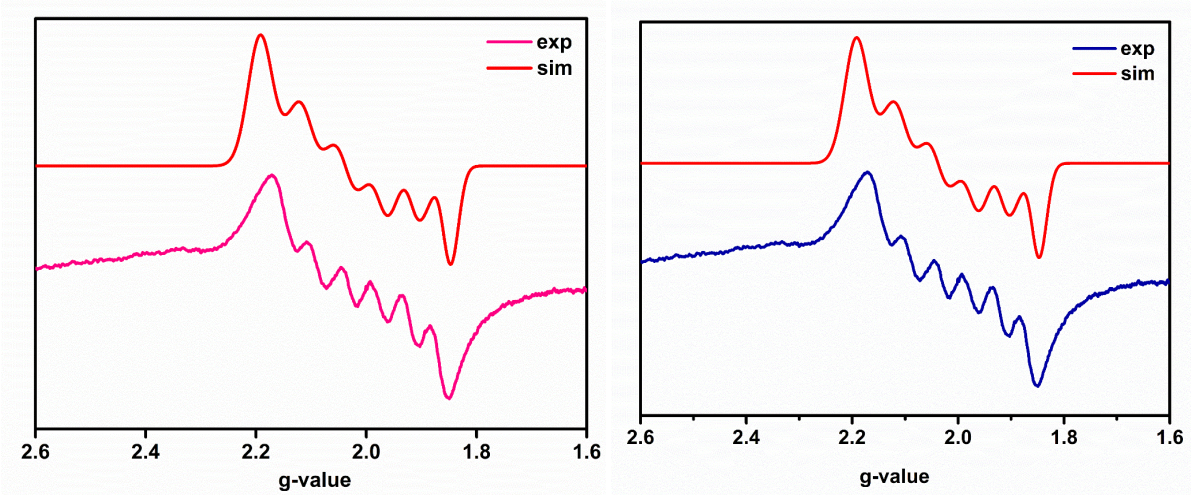

(a) **(b)**

Fig. S14. X-Band EPR spectra of complexes (a) **1** and (b) **2** in 1:1(v/v) methanol-water medium at 77 K.

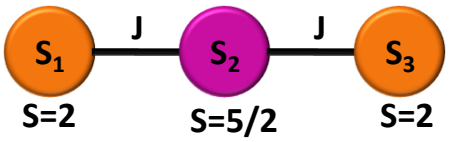

Fig. S15. Model used to fit the $\chi_M T$ vs. T plot of complexes **1** and **2**.

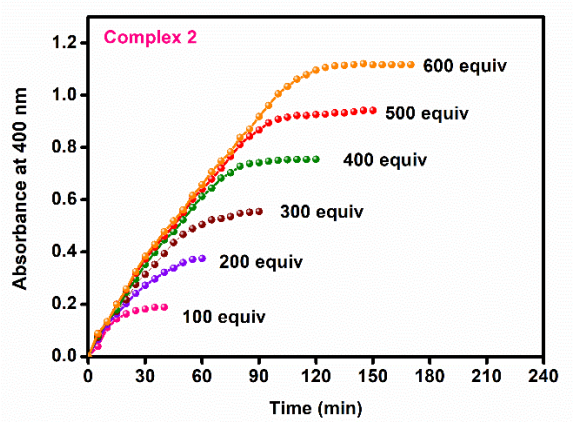

Fig. S16. Increased absorbance at 400 nm at different substrate concentrations catalyzed by complex **2** in acetonitrile medium at 25 °C.

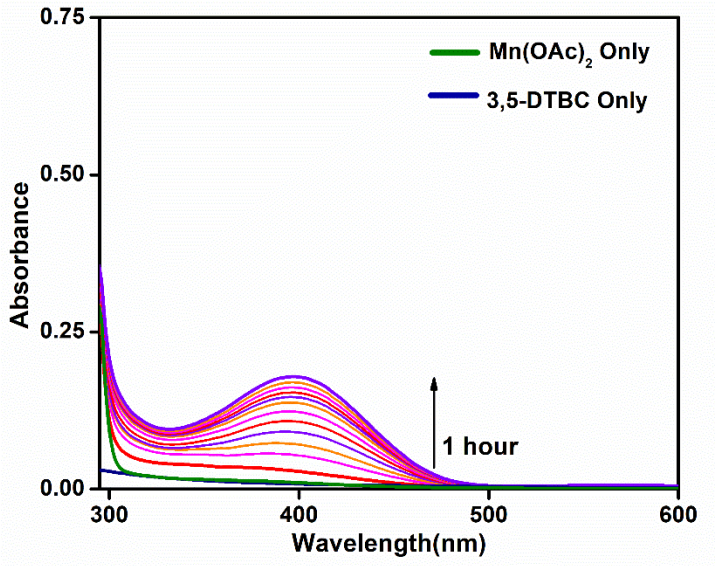

Fig. S17 Oxidation of 3,5-DTBC catalyzed by manganese(II) acetate monitored by UV-Vis spectroscopy in acetonitrile medium at 25 °C.

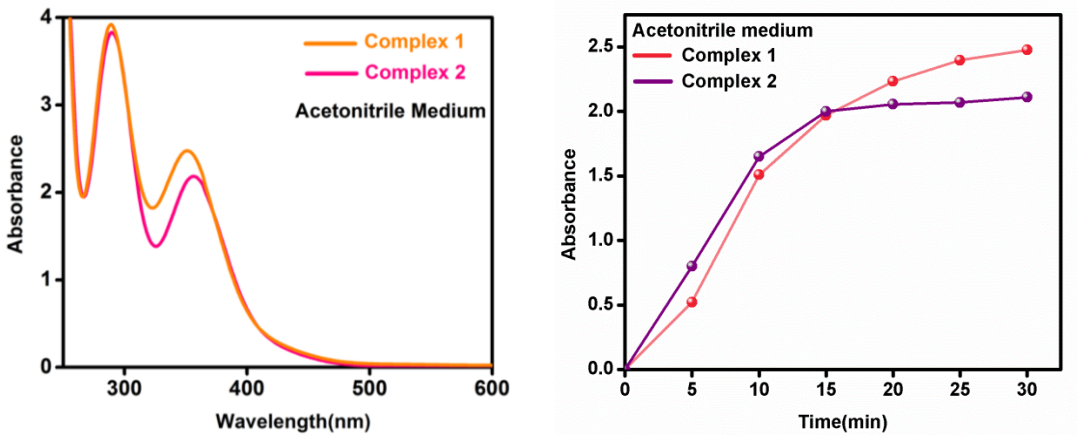

(a) (b)

Fig. S18. (a) Detection of H_2O_2 by UV-Vis spectroscopy during oxidation of 3,5-DTBC catalyzed by complexes **1** and **2** in acetonitrile; (b) Release of H_2O_2 during the catalytic reaction for complexes **1** and **2** in acetonitrile. The change in absorbance with time was measured at λ_{max} ~ 351 and 356 nm for **1** and **2**, respectively.

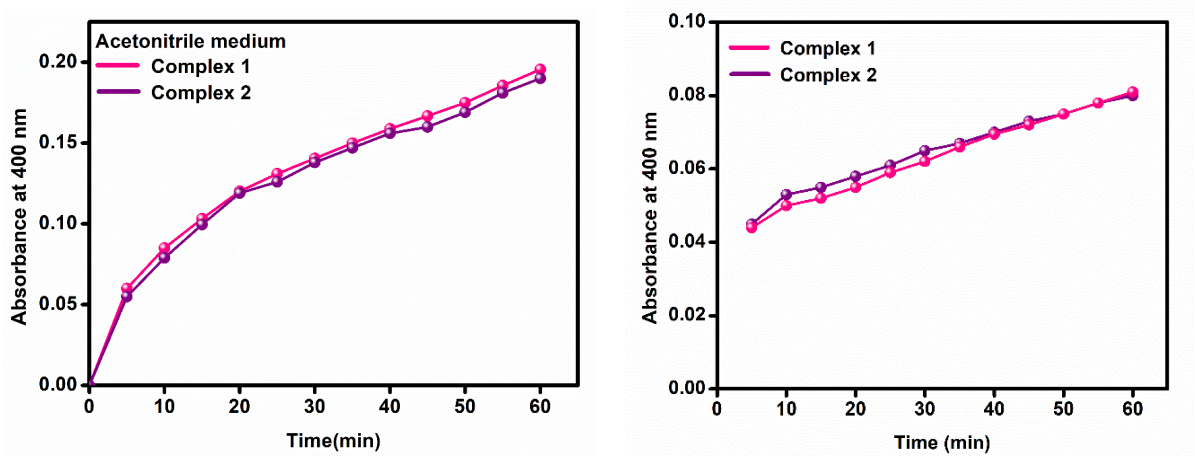

(a) **(b)**

Fig. S19. Monitoring of absorbance at 400 nm in the presence of (a) TEMPO and (b) sodium azide through the catalysis with complexes **1** and **2.**

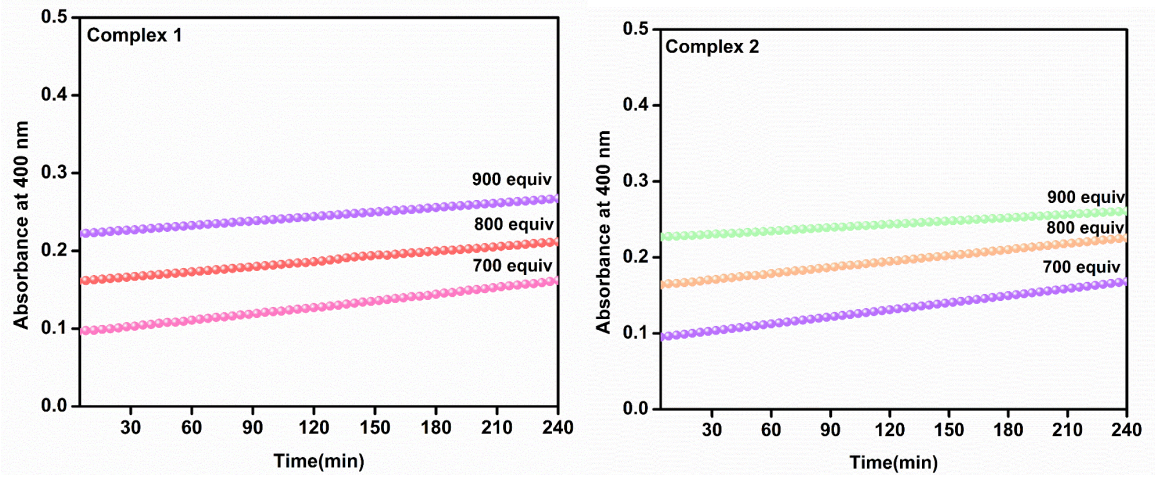

Fig. S20. Increasing absorbance at 400 nm at different substrate concentrations (higher than 600 equivalents) through the catalysis with complexes **1** and **2** in acetonitrile at 25 °C.

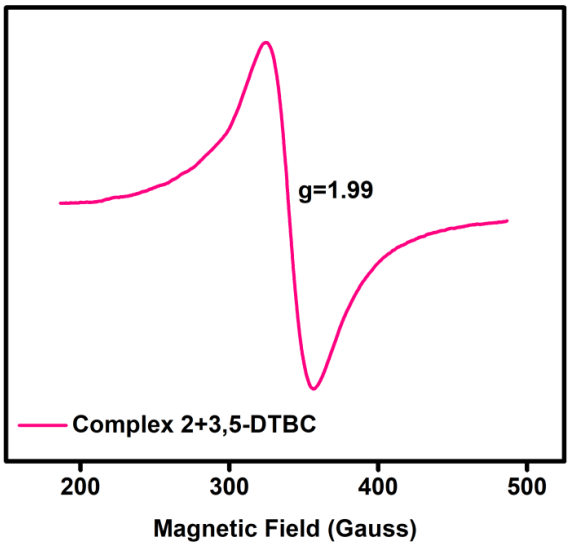

Fig. S21. X-Band EPR spectrum of complex **2** in the presence of 3,5-DTBC in acetonitrile at 77 K.

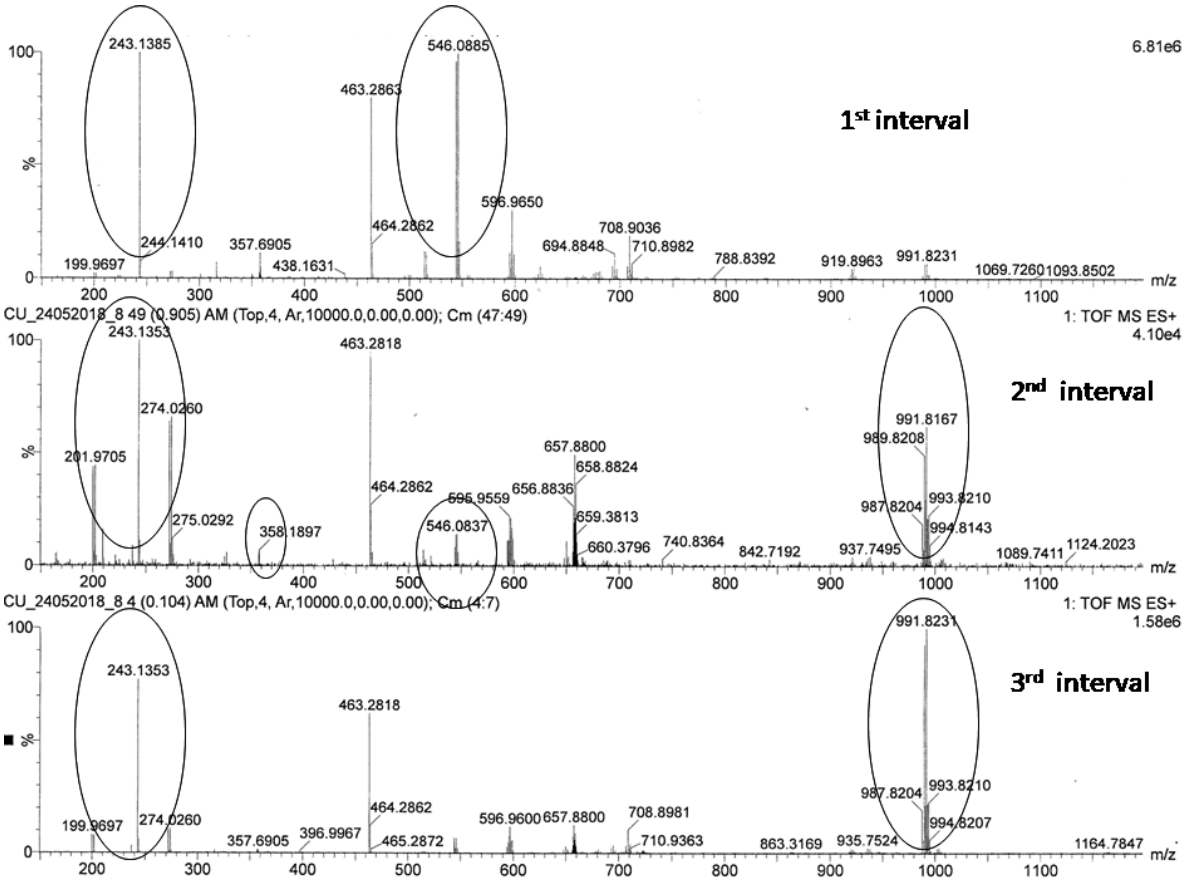

Fig. S22. ESI-MS spectrum of the reaction mixture of complex **1** and 3,5-DTBC in acetonitrile medium at a different time interval.

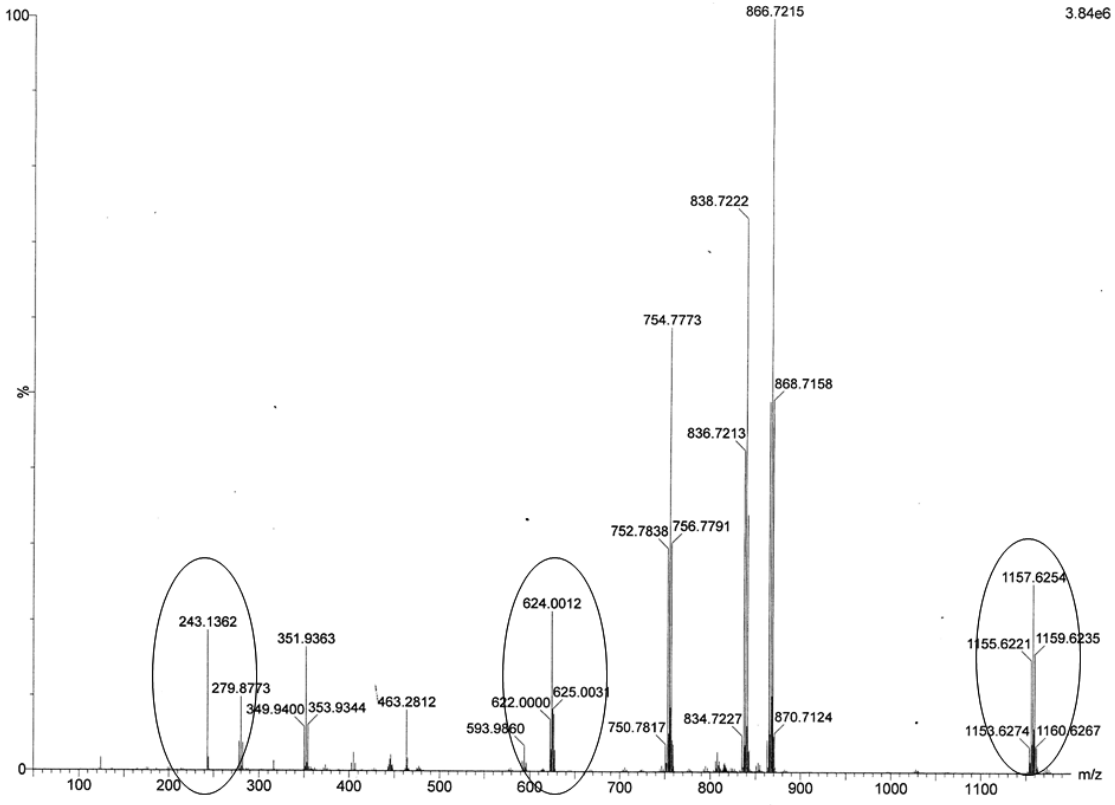

Fig. S23. ESI-MS spectrum of the reaction mixture of complex **2** and 3,5-DTBC in acetonitrile.

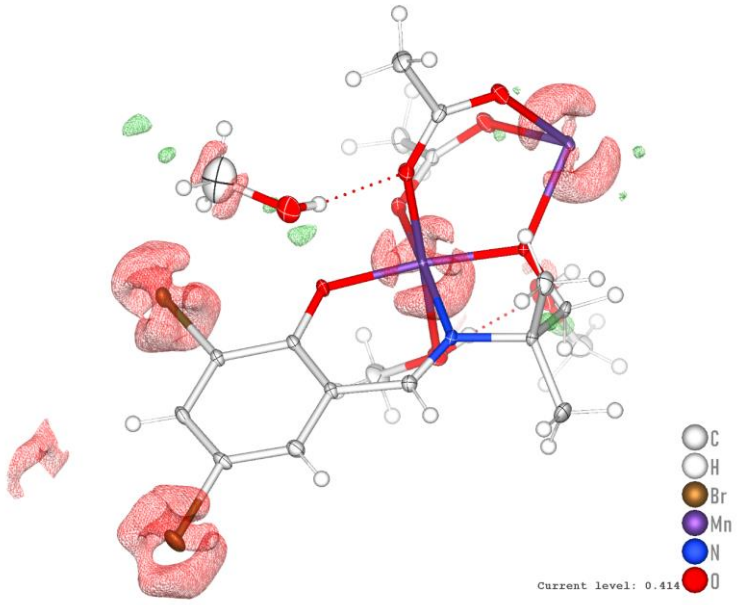

Fig. S24. Residual density map of complex **2.**

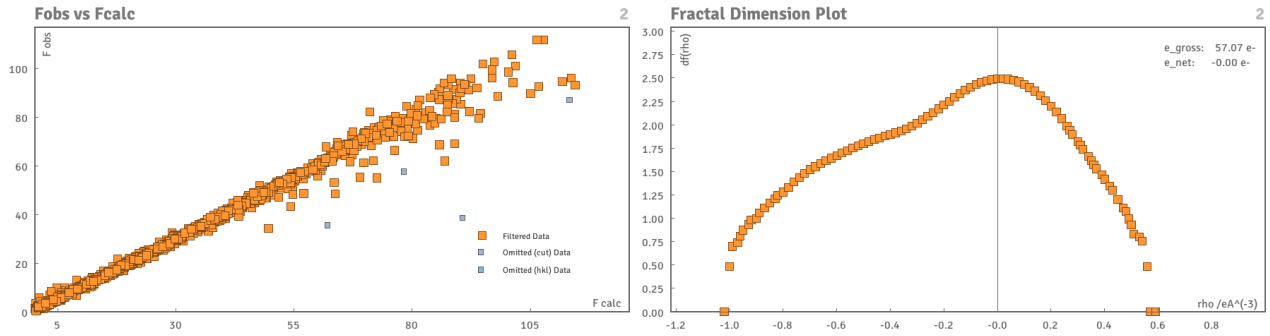

Fig. S25. Fobs *vs* Fcalc and Fractal Dimension Plot of complex **2**. (According to K. Meindl and J. Henn (2008), Acta Cryst. A64, 404-418)